



Deformed shapes of axisymmetric capsules enclosed by elastic membranes

C. POZRIKIDIS

Department of Mechanical and Aerospace Engineering, University of California, San Diego, La Jolla, California 92093-0411, USA (e-mail: cpozrikidis@ucsd.edu; Internet: <http://stokes.ucsd.edu>)

Received 22 May 2002; accepted in revised form 20 September 2002

Abstract. A boundary-value problem is formulated describing the shapes of inflated and deflated axisymmetric capsules enclosed by elastic membranes. When the membrane tension is isotropic and the principal bending moments obey constitutive equations involving the principal curvatures in the reference and deformed state but not the stretch ratios, the capsule shape is governed by a third-order ordinary differential equation for the meridional curvature involving the difference between the internal and external pressure. Numerical solutions of the boundary-value problem illustrate the shape of deflated spherical capsules enclosed by incompressible membranes and the shape of inflated and deflated biconcave capsules resembling red blood cells. The results demonstrate that the solution space of deformed spherical capsules consists of bifurcating branches arising at a sequence of transmural pressures, and illustrate the pressure developing inside spherical and biconcave capsules when a certain amount of fluid has been injected into, or withdrawn from, the interior.

Key words: boundary-value problems, capsules, elastic shells, red blood cells

1. Introduction

Thin-shell theory provides us with a natural framework for describing the stationary shapes and the flow-induced deformation of industrial capsules and biological cells. In this formulation, the interfaces are regarded as distinct two-dimensional media embedded in three-dimensional space, developing tangential and transverse tensions and bending moments due to the deformation from a reference configuration. A variety of results may then be obtained regarding the geometry of equilibrium shapes, and the stability and finite deformation under the influence of a nonzero transmural pressure or due to the action of an externally imposed viscous flow. For example, thin-shell theory has been used to explain the biconcave shape of healthy red blood cells, to estimate the bending modulus of biological membranes aspirated into a micropipette in terms of the suction length, to describe the deformed capsule shapes of vesicles in various types of viscous flow, and to study the rheological properties of dispersions.

Of particular interest in this work are the equilibrium shapes of inflated and deflated capsules with axisymmetric resting shapes. This problem has been discussed extensively in the biomechanics literature with specific reference to the biconcave discoidal shape assumed by resting healthy red blood cells (e.g., [1]). A focal point of this discussion has been the question as to whether the natural biconcave shape is also a resting shape with vanishing membrane tensions and bending moments. If the unstressed shape of the cells is spherical, or if the membrane enclosing red blood cells has a tendency to become flat so as to minimize its configurational energy, then the pressure inside the cells must be lower than that on the outside. Even though the internal pressure is hard to measure in the laboratory and the origin of the

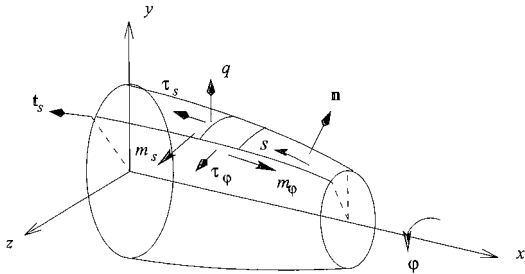


Figure 1. Illustration of an axisymmetric membrane showing the principal elastic tensions and bending moments.

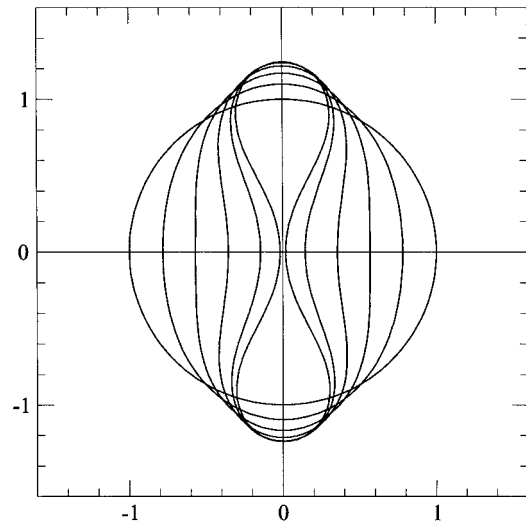


Figure 2. Contours of oblate and biconcave cells whose curvature is given by Equation (2.8) with $\delta = 0$ (sphere), 0.5, 1.0, 1.5, 2.0, and 2.3. The shapes have been scaled so that the cells have the same surface area.

biconcave shape remains unclear, an understanding of the functional relationship between the transmural pressure – defined as the difference between the interior cell and ambient pressure – and the cell volume for given surface area is useful for elucidating this important aspect of cell biomechanics.

Most relevant to this work are the computations of deflated and inflated capsules with spherical and biconcave resting shapes by Zarda *et al.* [4], to be discussed in more detail in Section 4. The numerical investigation of these authors appears to be the only theoretical study of finite capsule deformation in hydrostatics. Our approach parallels theirs in the early stages of the mathematical formulation by employing classical concepts of membrane or thin-shell theory, but then deviates in several important ways.

First, we show that, when the membranes tensions are isotropic and the principal bending moments obey constitutive equations involving the principal curvatures in the resting and deformed state, but not the stretch ratios, the capsule shape is governed by a third-order ordinary differential equation for the meridional curvature involving the transmural pressure. Isotropic tensions develop when the free energy of the membrane is a strong function of the rate of dilatation, as in the case of biological membranes consisting of lipid bilayers enclosing red blood cells. The differential equation for axisymmetric capsules derived in this paper is a generalization of that describing buckled shapes of two-dimensional (cylindrical) tubes enclosed by inextensible shells. Second, we demonstrate that the solution space of spherical resting capsules consists of bifurcated branches arising at a sequence of transmural pressures and corresponding to difference circumferential modes. The possibility of multiple solutions appears to have escaped the attention of previous authors. Third, we present accurate information on the pressure developing inside a deformed capsule when a certain amount of fluid has been injected into, or withdrawn from, the interior.

The main limitation of the present approach is the restriction on the class of constitutive equations for the elastic tensions and bending moments involving the curvatures. Although a generalization at the expense of computational efficiency is possible, it appears unlikely that capsules whose membrane material obeys different constitutive equations will show a significantly different qualitative behavior.

2. Mathematical formulation

Consider a liquid capsule enclosed by an axisymmetric membrane generated by rotating a curve around the x axis, and introduce polar cylindrical coordinates consisting of the axial position x , the distance from the x axis denoted by σ , and the meridional angle measured around the x axis with origin in the xy plane denoted by φ , as illustrated in Figure 1. The fluid stresses inside and outside the capsule and the membrane tensions and bending moments developing due to the deformation are all assumed to be axisymmetric.

Working under the auspices of thin-shell theory, we consider the mid-surface of the membrane and introduce the azimuthal and meridional tensions τ_s and τ_φ , which are the principal tensions of the in-plane stress resultants, the transverse shear tension q exerted on a cross-section of the membrane that is normal to the x axis, and the azimuthal and meridional bending moments m_s and m_φ , as depicted in Figure 1.

2.1. GEOMETRICAL PRELIMINARIES

To prepare the ground for the mathematical formulation, we introduce the arc length measured along the contour of the membrane in a meridional plane, denoted by s , and the unit vector that is tangential to the membrane and lies in a meridional plane defined by a certain value of the meridional angle φ , denoted by \mathbf{t}_s . The unit vector normal to the membrane, \mathbf{n} , points outward, as illustrated in Figure 1. The principal curvatures of the membrane in a meridional plane and its conjugate plane are denoted by κ_s and κ_φ .

Using fundamental relations of differential geometry, we find that, if the radial position of the membrane is described by the equations

$$\sigma = \sigma(s) = \Sigma(x), \quad (2.1)$$

then the principal curvatures are given by

$$\kappa_s = -\frac{\pm\sigma''}{\sqrt{1-\sigma'^2}} = -\frac{\pm\Sigma_{xx}}{(1+\Sigma_s^2)^{3/2}} \quad (2.2)$$

and

$$\kappa_\varphi = -\frac{1}{\sigma} \frac{dx}{ds} = \pm \frac{1}{\sigma} \sqrt{1-\sigma'^2} = \pm \frac{1}{\sigma \sqrt{1+\Sigma_x^2}}, \quad (2.3)$$

where $\sigma' \equiv d\sigma/ds$ and $\Sigma_x \equiv d\Sigma/dx$ (e.g., [5, p. 162]). The plus sign of \pm is selected when $dx/ds < 0$, and the minus sign otherwise.

Expressions (2.2) and (2.3) are consistent with Codazzi's equation

$$\kappa_s = \frac{d(\sigma\kappa_\varphi)}{d\sigma}, \quad (2.4)$$

which allows us to compute one of the principal curvatures in terms of the other (e.g., [6, p. 9]). Rearranging (2.4), we obtain

$$\frac{d\kappa_\varphi}{d\sigma} = \frac{\kappa_s - \kappa_\varphi}{\sigma}. \quad (2.5)$$

Applying now (2.5) at the axis of symmetry, $\sigma = 0$, and using the rule de l'Hôpital to evaluate the right-hand side, we obtain $2(d\kappa_\varphi/ds)_{\sigma=0} = (d\kappa_s/ds)_{\sigma=0}$. Differentiating (2.5) with respect to s and working in a similar fashion, we find $3(d^2\kappa_\varphi/ds^2)_{\sigma=0} = (d^2\kappa_s/ds^2)_{\sigma=0}$.

To compute the contour of a capsule in terms of the curvature $\kappa_s(s)$, we regard the x and σ coordinates of point particles along the trace of the membrane in a meridional plane as functions of the meridional arc length s , writing $x = x_1(s)$ and $\sigma = \sigma(s) \equiv x_2(s)$. By definition then, $x_1'^2 + x_2'^2 = 1$, which can be differentiated to yield $x_1'x_1'' = -x_2'x_2''$, where a prime denotes a derivative with respect to s . Using elementary differential geometry, we derive the relations

$$\kappa_s = -x_1''x_2' + x_1'x_2'' = -\frac{x_1''}{x_2'} = \frac{x_2''}{x_1'}. \quad (2.6)$$

Next, we introduce the functions $x_3 \equiv x_1'$ and $x_4 \equiv x_2'$ satisfying $x_3^2 + x_4^2 = 1$, and obtain the following system of four nonlinear differential equations,

$$\frac{dx_1}{ds} = x_3, \quad \frac{dx_2}{ds} = x_4, \quad \frac{dx_3}{ds} = -\kappa_s x_4, \quad \frac{dx_4}{ds} = \kappa_s x_3. \quad (2.7)$$

The second pair of equations is decoupled from the first pair and can be integrated independently. Once the solution has been found, the first pair can be integrated to produce the shell shape.

For example, to compute an oblate or biconcave shape that is symmetric with respect to the mid-plane $x = 0$, as illustrated in Figure 2, we may express the meridional curvature in the form

$$\kappa_s = \frac{\pi}{L} \left(1 - \delta \cos \frac{\pi s}{L}\right), \quad (2.8)$$

where $0 \leq s \leq L$, L is the total arc length of the cell contour in a meridional plane, and δ is a specified dimensionless amplitude, and then integrate system (2.7) using, for example, a Runge-Kutta method (e.g., [7]) with initial conditions

$$x_1(0) = x_0, \quad x_2(0) = 0, \quad x_3(0) = 0, \quad x_4(0) = 1, \quad (2.9)$$

where x_0 is an arbitrary position. Cell contours computed in this manner are displayed in Figure 2 for $\delta = 0$ (sphere), 0.5, 1.0, 1.5, 2.0, and 2.3, on a scale that has been adjusted so that all cells have the same surface area. The shape for $\delta = 2.0$ is similar to the average shape of normal blood cells reported by Evans and Fung [8].

2.2. FORCE AND TORQUE BALANCES

Equilibrium equations can be derived by considering a small section of the membrane that is confined between (a) two adjacent meridional planes passing through the x axis, and (b) two parallel planes that are perpendicular to the x axis and enclose a small section of the membrane in a meridional plane, as depicted in Figure 1. Performing a force balance over this section, we find that the jump in the traction across the membrane is given by

$$\Delta \mathbf{f} = (\boldsymbol{\sigma}^{(s)} - \boldsymbol{\sigma}^{(c)}) \cdot \mathbf{n} = \Delta f^n \mathbf{n} + \Delta f^s \mathbf{t}_s, \quad (2.10)$$

where $\sigma^{(s)}$ is the stress tensor in the surrounding fluid, and $\sigma^{(c)}$ is the stress tensor inside the cell. The normal jump is given by

$$\Delta f^n = \kappa_s \tau_s + \kappa_\varphi \tau_\varphi - \frac{d}{ds}(\sigma q), \quad (2.11)$$

and the tangential jump is given by

$$\begin{aligned} \Delta f^s &= -\frac{d\tau_s}{ds} - \frac{1}{\sigma} \frac{d\sigma}{ds} (\tau_s - \tau_\varphi) - \kappa_s q \\ &= -\frac{1}{\sigma} \frac{d(\sigma \tau_s)}{ds} + \frac{\tau_\varphi}{\sigma} \frac{d\sigma}{ds} - \kappa_s q. \end{aligned} \quad (2.12)$$

An analogous torque balance relates the transverse shear tension to the bending moments by

$$q = \frac{1}{\sigma} \left(\frac{d(\sigma m_s)}{ds} - m_\varphi \frac{d\sigma}{ds} \right) = \frac{1}{\sigma} \frac{d\sigma}{ds} \left(\frac{d(\sigma m_s)}{d\sigma} - m_\varphi \right), \quad (2.13)$$

(e.g., [6, p. 33]). Substituting the right-hand side of (2.13) in place of the shear tension in (2.11) and (2.12), we obtain expressions for the jump in traction in terms of the in-plane tensions and bending moments alone.

2.3. CONSTITUTIVE EQUATIONS FOR THE ELASTIC TENSIONS

To develop constitutive equations for the elastic tensions, we introduce the principal extension ratios

$$\lambda_s = \frac{ds}{ds_R}, \quad \lambda_\varphi = \frac{\sigma}{\sigma_R}, \quad (2.14)$$

where the subscript R , subsequently also used as a superscript, denotes a reference state. If the area of the membrane is locally and thus globally conserved, $\lambda_s \lambda_\varphi = 1$. To this end, we have two main choices reflecting the assumed nature of the membrane.

First, we may regard the membrane as a distinct two-dimensional elastic medium and express the principal stress resultants in terms of the *surface* strain energy function or Helmholtz free surface energy W_S . Alternatively, we may regard the membrane as a thin sheet of a three-dimensional incompressible material, and express the principal stress resultants in terms of a *volume* strain energy function W_V . The proper choice depends on the membrane constitution.

2.4. CONSTITUTIVE EQUATIONS FOR THE BENDING MOMENTS

To compute the bending moments developing in an elastic membrane, we may introduce the bending measures of strain

$$K_s = \lambda_s \kappa_s - \kappa_s^R, \quad K_\varphi = \lambda_\varphi \kappa_\varphi - \kappa_\varphi^R, \quad (2.15)$$

(e.g., [4], [9–12]). The bending moments may then be expressed in terms of the surface bending strain energy function W_B as

$$m_s = \frac{1}{\lambda_\varphi} \frac{\partial W_B}{\partial K_s}, \quad m_\varphi = \frac{1}{\lambda_s} \frac{\partial W_B}{\partial K_\varphi}. \quad (2.16)$$

Love's first approximation is expressed by the quadratic form

$$W_B = \frac{1}{2}E_B(K_s^2 + 2\nu K_s K_\varphi + K_\varphi^2). \quad (2.17)$$

Substituting (2.17) in (2.16), we find

$$m_s = \frac{E_B}{\lambda_\varphi}(K_s + \nu K_\varphi), \quad m_\varphi = \frac{E_B}{\lambda_s}(K_\varphi + \nu K_s). \quad (2.18)$$

The bending measures (2.15) have been designed so that self-similar deformations do not induce bending moments; an example is provided by the expansion of a sphere. This choice is appropriate for molecular membranes whose bending moments depend exclusively on the solid angles of the molecular bonds. For membranes comprised of thin elastic sheets whose thickness changes as a result of the deformation, we may replace the constitutive equations (2.18) with the alternative linear relations

$$m_s = E_B(\kappa_s - \kappa_s^R), \quad m_\varphi = E_B(\kappa_\varphi - \kappa_\varphi^R). \quad (2.19)$$

In the case of a spherical membrane with reference radius a_R and deformed radius a , equations (2.19) yield $m_s = m_\varphi = \frac{E_B}{a_R \lambda}(1 - \lambda)$, where $\lambda \equiv a/a_R$ is the extension ratio. Note that the bending moments are negative in the case of expansion and positive in the case of shrinkage.

An in-depth discussion of constitutive equations for the bending moments has been given by Steigmann and Ogden [13–15].

2.5. CAPSULE SHAPES IN HYDROSTATICS

Consider now the equilibrium shape of a deformed axisymmetric capsule enclosed by an elastic membrane in hydrostatics. When the effects of gravity are insignificant, the pressure inside and outside the capsule is constant denoted, respectively, by p_c and p_s . Setting $\boldsymbol{\sigma}^{(s)} = -p_s \mathbf{I}$ and $\boldsymbol{\sigma}^{(c)} = -p_c \mathbf{I}$, where \mathbf{I} is the identity matrix, we find that the jump in hydrodynamic traction across the membrane is given by $\Delta \mathbf{f} = \Delta p_t \mathbf{n}$, where $\Delta p_t \equiv p_c - p_s$ is the transmural pressure. The equilibrium equations (2.11) and (2.12) require

$$\kappa_s \tau_s + \kappa_\varphi \tau_\varphi - \Delta p_t = \frac{1}{\sigma} \frac{d(\sigma q)}{ds} \quad (2.20)$$

and

$$\frac{d(\sigma \tau_s)}{ds} - \tau_\varphi \frac{d\sigma}{ds} = -\sigma \kappa_s q, \quad (2.21)$$

where the transverse shear tension q is given in terms of the bending moments by (2.13). In the case of spherical capsule of radius a , equal principal curvatures $\kappa_s = \kappa_\varphi = 1/a$ and mean curvature $\kappa_m = 1/a$, Equations (2.20) and (2.21) are clearly satisfied by Laplace's formula $\tau_s = \tau_\varphi = \Delta p_t / (2\kappa_m)$ and $q = 0$.

When the membrane tensions are isotropic, $\tau_s = \tau_\varphi = \gamma$, Equations (2.20) and (2.21) obtain the simplified forms

$$2\gamma \kappa_m = \Delta p_t + \frac{1}{\sigma} \frac{d(\sigma q)}{ds}, \quad \frac{d\gamma}{ds} = -\kappa_s q, \quad (2.22)$$

where $\kappa_m = \frac{1}{2}(\kappa_s + \kappa_\varphi)$ is the mean curvature. Solving the first equation in (2.22) for γ and substituting the result in the second equation, we obtain

$$\frac{d}{ds} \left[\frac{1}{2\kappa_m} \left(\frac{1}{\sigma} \frac{d(\sigma q)}{ds} + \Delta p_t \right) \right] + \kappa_s q = 0. \quad (2.23)$$

It is convenient for computational purposes to introduce the reduced tension $w(s) \equiv \gamma(s)/E_B$ satisfying the differential equation

$$\frac{dw}{ds} = -\frac{1}{E_B} \kappa_s q = -\frac{1}{E_B} \frac{\kappa_s}{\sigma} \left(\frac{d(\sigma m_s)}{ds} - m_\varphi \frac{d\sigma}{ds} \right), \quad (2.24)$$

where E_B is a constant bending modulus. The right-hand side of (2.24) arises by expressing the transverse shear tension in terms of the bending moments using the equilibrium equation (2.13). The first of equations (2.22) yields

$$\frac{d(\sigma q)}{ds} + \sigma \Delta p_t - 2E_B \kappa_m \sigma w(s) = 0. \quad (2.25)$$

To this end, we adopt the constitutive equations (2.19), and recast (2.24) and (2.25) into the more specific form

$$\frac{dw}{ds} = -\frac{\kappa_s}{\sigma} \left(\frac{d[\sigma(\kappa_s - \kappa_s^R)]}{ds} - (\kappa_\varphi - \kappa_\varphi^R) \frac{d\sigma}{ds} \right), \quad (2.26)$$

and

$$\frac{d^2[\sigma(\kappa_s - \kappa_s^R)]}{ds^2} - \frac{d}{ds} [(\kappa_\varphi - \kappa_\varphi^R) \frac{d\sigma}{ds}] + \sigma \frac{\Delta p_t}{E_B} - 2\kappa_m \sigma w(s) = 0. \quad (2.27)$$

Isolating the terms containing the reference curvatures on the right-hand side and rearranging, we obtain

$$\begin{aligned} \frac{dw}{ds} + \kappa_s \left(\frac{d\kappa_s}{ds} + \frac{1}{\sigma} \frac{d\sigma}{ds} (\kappa_s - \kappa_\varphi) \right) &= \frac{dw}{ds} + 2\kappa_s \frac{d\kappa_m}{ds} \\ &= \kappa_s \left(\frac{d\kappa_s^R}{ds} + \frac{1}{\sigma} \frac{d\sigma}{ds} (\kappa_s^R - \kappa_\varphi^R) \right), \end{aligned} \quad (2.28)$$

$$\begin{aligned} \frac{d^2(\sigma \kappa_s)}{ds^2} - \frac{d}{ds} (\kappa_\varphi \frac{d\sigma}{ds}) + \sigma \frac{\Delta p_t}{E_B} - 2\kappa_m \sigma w(s) \\ = (\kappa_s^R - \kappa_\varphi^R) \frac{d^2\sigma}{ds^2} + \frac{d(2\kappa_s^R - \kappa_\varphi^R)}{ds} \frac{d\sigma}{ds} + \sigma \frac{d^2\kappa_s^R}{ds^2}. \end{aligned} \quad (2.29)$$

The second expression in (2.28) was derived with the help of (2.5). When the reference shape of the shell is a sphere of radius a_R , $\kappa_s^R = \kappa_\varphi^R = 1/a_R$ the right-hand sides of (2.28) and (2.29) vanish, and the resulting simplified equations are distinguished by the absence of the reference curvature.

Eliminating the reduced tension $w(s)$ from (2.26) and (2.27), we obtain a third-order differential equation for the curvatures with respect to the meridional arc length,

$$\begin{aligned} \frac{d}{ds} \left[\frac{1}{2\kappa_m \sigma} \left(\frac{d^2[\sigma(\kappa_s - \kappa_s^R)]}{ds^2} - \frac{d}{ds} [(\kappa_\varphi - \kappa_\varphi^R) \frac{d\sigma}{ds}] + \sigma \frac{\Delta p_t}{E_B} \right) \right] \\ + \frac{\kappa_s}{\sigma} \left(\frac{d[\sigma(\kappa_s - \kappa_s^R)]}{ds} - (\kappa_\varphi - \kappa_\varphi^R) \frac{d\sigma}{ds} \right) = 0. \end{aligned} \quad (2.30)$$

Far from the axis of symmetry, κ_φ and κ_φ^R tend to vanish, and (2.30) takes the simplified asymptotic form

$$\frac{d}{ds} \left[\frac{1}{\kappa_s} \left(\frac{d^2(\kappa_s - \kappa_s^R)}{ds^2} + \frac{\Delta p_t}{E_B} \right) \right] + \kappa_s \frac{d(\kappa_s - \kappa_s^R)}{ds} = 0, \quad (2.31)$$

involving only the meridional curvature in the deformed and reference state. Equation (2.31) is the point of departure for computing the buckled shapes of two-dimensional (cylindrical) cells under a negative transmural pressure *e.g.*, [16, 17]).

Given the distribution of the reference curvatures around the deformed contour, $\kappa_s^R(s)$ and $\kappa_\varphi^R(s)$, Equations (2.2), (2.3), (2.7), (2.28) and (2.29) provide us with a complete system of coupled ordinary differential equations for the functions $x_1(s)$, $x_2(s)$, $x_3(s)$, $x_4(s)$, $\kappa_s(s)$, $\kappa_\varphi(s)$, and $w(s)$. An equivalent system of first-order equations arises by recalling the definitions $x = x_1(s)$, $\sigma = x_2(s)$, denoting $\kappa_s \equiv x_5(s)$, $dx_5/ds \equiv x_6(s)$, and $w = x_7(s)$, and collecting the governing equations into the system

$$\frac{dx_i}{ds} = f_i, \quad (2.32)$$

for $i = 1, \dots, 7$. Using equation (2.3) to write $\kappa_\varphi = -x_3/x_2$ and Codazzi's equation (2.5) to write $d\kappa_\varphi/ds = x_4(x_2x_5 + x_3)/x_2^2$, we find that the phase-space velocities are given by

$$\begin{aligned} f_1 &= x_3, & f_2 &= x_4, & f_3 &= -x_5x_4, & f_4 &= x_5x_3, & f_5 &= x_6, \\ f_6 &= -2\frac{x_4x_6}{x_2} + \left(\frac{x_4^2}{x_2^2} - \frac{x_3x_5}{x_2}\right)(x_5 + \frac{x_3}{x_2}) - \frac{\Delta p_t}{E_B} + (x_5 - \frac{x_3}{x_2})x_7 \\ &\quad + (\kappa_s^R - \kappa_\varphi^R)\frac{x_5x_3}{x_2} + \frac{x_4}{x_2} \left(2\frac{d\kappa_s^R}{ds} - \frac{d\kappa_\varphi^R}{ds} \right) + \frac{d^2\kappa_s^R}{ds^2}, \\ f_7 &= -x_5 \left[x_6 + \frac{x_4}{x_2} \left(x_5 + \frac{x_3}{x_2} \right) - \frac{d\kappa_s^R}{ds} - \frac{x_4}{x_2} (\kappa_s^R - \kappa_\varphi^R) \right]. \end{aligned} \quad (2.33)$$

The accompanying boundary conditions are: $x_1(0) = x_0$, $x_2(0) = 0$, $x_3(0) = 0$, $x_4(0) = 1$, $x_6(0) = 0$ at the axis of symmetry, $s = 0$ and $\sigma = 0$, where x_0 is an arbitrary position along the x axis. For shapes with left-to-right symmetry, such as those depicted in Figure 2, we also require $x_4(L/2) = 0$ and $x_6(L/2) = 0$, where L is the total arc length of the contour of the membrane in a meridional plane.

The expressions for the phase-space velocities f_6 and f_7 become indeterminate at the axis of symmetry where $\sigma \equiv x_2 = 0$. Careful consideration of the limit of the corresponding differential equations assisted by Codazzi's equations (2.4) and (2.5) shows that

$$f_6(0) = -\frac{3}{8} \left(\frac{\Delta p_t}{E_B} - 2\kappa_s(0)x_7(0) \right) + \frac{9}{8} \frac{d^2\kappa_s^R}{ds^2} - \frac{3}{8} \frac{d^2\kappa_\varphi^R}{ds^2}, \quad f_7(0) = 0. \quad (2.34)$$

In the space of dimensionless functions, the solution of system (2.32) can be parametrized by one of the dimensionless negative transmural pressures

$$\Delta \hat{p}_L \equiv \frac{\Delta p_t}{\kappa_L^3 E_B}, \quad \Delta \hat{p}_S \equiv \frac{\Delta p_t}{\kappa_S^3 E_B}, \quad \Delta \hat{p}_V \equiv \frac{\Delta p_t}{\kappa_V^3 E_B}, \quad (2.35)$$

where $\kappa_L = 1/a_L$ is the mean curvature of the equivalent spherical shape whose perimeter P in a meridional plane is equal to that of the capsule, $P = \pi a_L$; $\kappa_S = 1/a_S$ is the mean curvature of the equivalent spherical shape whose surface area S is identical to that of the capsule, $S = 4\pi a_S^2$; and $\kappa_V = 1/a_V$ is the mean curvature of the equivalent spherical shape whose volume V is same as that of the capsule, $V = \frac{4\pi}{3}a_V^3$. In practice, a family of solutions can be found by specifying the perimeter L , the curvature of the capsule at the axis of symmetry, $x_5(0)$, and the bending modulus, E_B , and then solving the boundary-value problem by the shooting method, where the trial variables are the transmural pressure and the initial value $x_7(0)$.

A numerical method was implemented for solving system (2.32) by the fourth-order Runge-Kutta method. The shooting variables were corrected by Newton's method, and the 2×2 Jacobian was computed by numerical differentiation. The solution of the boundary-value problem for each set of parameters requires only a few seconds of CPU time on a 1.7 GHz Intel processor running LINUX. Because multiple solution branches exist for a specified set of conditions, as will be discussed in Section 3, the converged capsule shape can be extremely sensitive to the initial guesses for the transmural pressure and to the value of $x_7(0)$. At high transmural pressures, parameter continuation with a very small step is necessary to successfully trace a branch.

3. Results

Consider first the deformation of a capsule with a spherical resting shape. The solid lines in Figure 3(a) show a family of oblate and dimpled deformed shapes for centerline curvature $a_L\kappa_s(0) = 0.99, 0.95, 0.90, 0.80, \dots, -1.00$, plotted on a scale that has been adjusted so that all capsules have the same surface area. The continuation of this family to shapes with lower negative centerline curvature yields unphysical self-intersecting capsules, as shown by the dashed line in Figure 3(a) corresponding to $a_L\kappa_s(0) = -1.40$. Half of these intersecting shapes, however, can be identified with a deformed hemispherical cap fitted to the end of a semi-infinite circular tube, buckling inward due to a difference between the low tube pressure and high ambient pressure. Figure 3(b) shows a second family of deformed shapes with more convoluted geometry for centerline curvature $a_L\kappa_s(0) = 0.98, 0.95, 0.90, 0.80, 0.60, \dots, -3.40, -3.60$.

Figure 4 displays the volume of the first and second family of shapes drawn, respectively, with thin and thick lines, plotted against the reduced centerline curvature $a_L\kappa_s(0)$. The solid lines show the volume normalized by $\frac{4\pi}{3}a_L^3$, and the dashed lines show the volume normalized by $\frac{4\pi}{3}a_S^3$. The information presented in this figure may be used to identify the shape of a spherical capsule after a certain amount of fluid has been withdrawn from its interior with a syringe, or diffused through the membrane. The results reveal that the volume of a cell enclosed by an incompressible membrane with constant surface area, such as the membrane of a vesicle enclosed by a lipid bilayer, decreases monotonically at a nearly quadratic rate with respect to the deviation of the centerline curvature from the reference value.

Given the ambient pressure, the interior capsule pressure and thus the transmural pressure is different for each one of the shapes displayed in Figure 3. Figure 5 shows a graph of the negative of the reduced transmural pressure $\Delta\hat{p}_L$ (solid line) and $\Delta\hat{p}_S$ (dashed line) defined in (2.35), plotted against the reduced centerline curvature $a_L\kappa_s(0)$. The results reveal that the spherical shape corresponding to $a_L\kappa_s(0) = 1$ is possible for any value of the transmural pres-

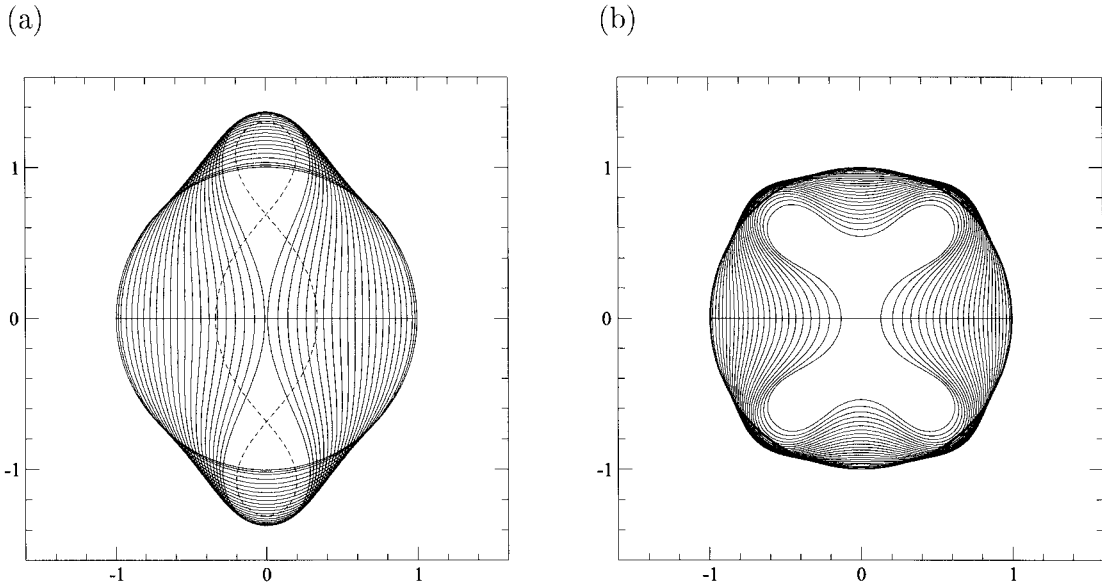


Figure 3. Two families of deformed shapes of a capsule with spherical resting shape for reduced centerline curvature (a) $a_L \kappa_s(0) = 0.99, 0.95, 0.9, 0.8, \dots, -1.0$, and (b) $0.98, 0.95, 0.90, 0.80, 0.60, \dots, -3.40, -3.60$. The dashed line in (a) shows a self-intersecting shape with $a_L \kappa_s(0) = -1.40$. The scale in both figures has been adjusted so that all capsules have the same surface area.

sure. Bifurcations into the first and second family of deformed shapes displayed in Figure 3 occur at the critical points $-(\Delta \hat{p}_L)_{cr} \simeq -(\Delta \hat{p}_S)_{cr} = 8$ and 36 .

The structure of the solution space displayed in Figure 5 is similar to that of a cylindrical elastic tube with a circular resting shape buckling inwards due to low tube pressure. In the case of the tube, bifurcating solution branches are known to originate from the critical transmural pressures $-\frac{\Delta p_r}{E_B \kappa_u^3} \equiv n^2 - 1$, where κ_u is the curvature of the undeformed shape and n is the wave number of the circumferential mode (e.g., [2, 17, 18]). The two solution branches displayed in Figure 3 correspond to the meridional modes $n = 2$ and 4 . The present numerical results suggest that the critical bifurcation points for a spherical cell are given by the formula $-(\Delta \hat{p}_L)_{cr} = 2(n^2 + n - 2)$.

More direct information on the transmural pressure of deflated capsules is presented in Figure 6, showing a graph of the negative of the transmural pressure $\Delta \hat{p}_S$ for the first and second family of shapes, drawn, respectively, with the thin and thick line, plotted against the capsule volume reduced so that all shapes have the same surface area. These results clearly demonstrate that withdrawing an infinitesimal amount of fluid from the capsule causes the internal pressure to assume quantum levels according to the prevailing mode of deformation. Although a rigorous proof is not available, the first mode corresponding to the biconcave shape is most likely to occur in practice.

To compute deformed shapes of capsules with non-spherical resting shapes, we must have available the distribution of the reference curvatures $\kappa_s^R(s)$ and $\kappa_\phi^R(s)$, where s is the arc length around the deformed contour. In general, to obtain these functions, it is necessary to introduce constitutive equations for the elastic tensions and simultaneously solve for the principal extension ratios. Doing this considerably complicates the mathematical formulation

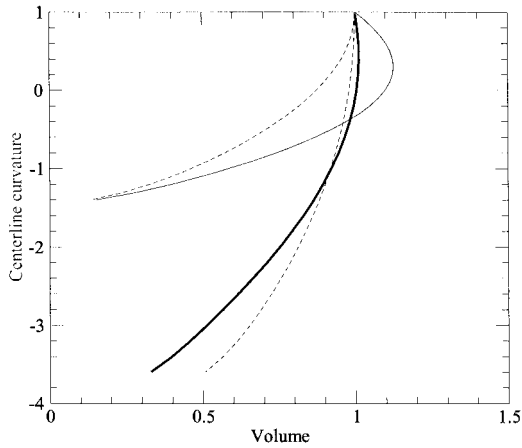


Figure 4. Volume of the first (thin lines) and second (thick lines) family of shapes displayed in Figure 3, plotted against the reduced centerline curvature $a_L \kappa_s(0)$. The solid lines show the volume normalized by $\frac{4\pi}{3} a_L^3$, and the dashed lines show the volume normalized by $\frac{4\pi}{3} a_S^3$.

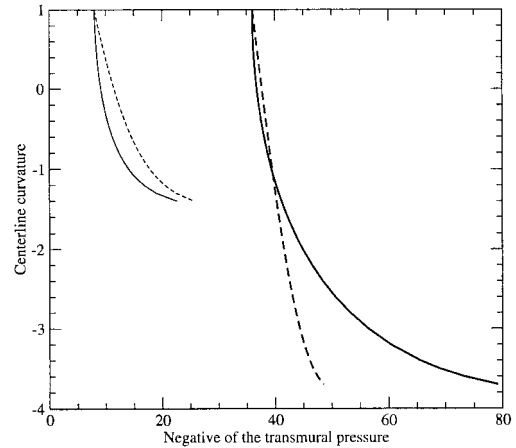


Figure 5. The vertical axis measures the reduced centerline curvature $a_L \kappa_s(0)$, and the horizontal axis measures the negative of the dimensionless transmural pressure $\Delta \hat{p}_L$ (solid lines) or $\Delta \hat{p}_S$ (dashed lines) defined in (2.35) for capsules with spherical undeformed shapes.

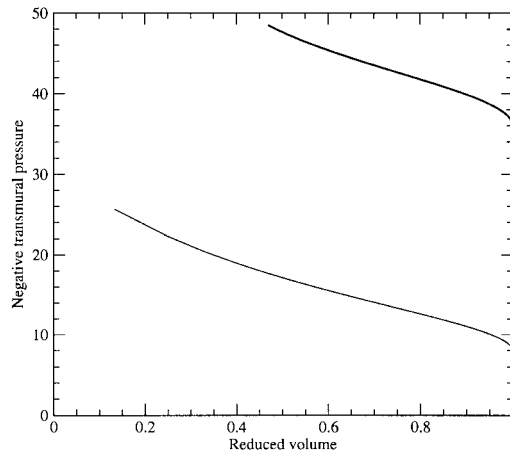


Figure 6. Negative of the transmural pressure $\Delta \hat{p}_S$ plotted against the capsule volume for the first (thin line) and second (thick line) family of deformed shapes displayed in Figure 3.

by introducing further terms containing the principal stretch ratios in the governing equations (2.33).

As a compromise, we assume that $\lambda_s = 1$, and therefore $\kappa_s^R(s) = \kappa_s^R(s_R)$ and $\kappa_\varphi^R(s) = \kappa_\varphi^R(s_R)$, whereupon the meridional arc lengths s and s_R vary over the same range. Conversely, this assumption may be regarded as an artificial constitutive equation that can be used to make a correspondence between the position of point particles in the reference and deformed state. When the incompressibility constraint $\lambda_s \lambda_\varphi = 1$ is also required, $\lambda_\varphi = 1$, and point particles along the membrane are displaced parallel to the x axis.

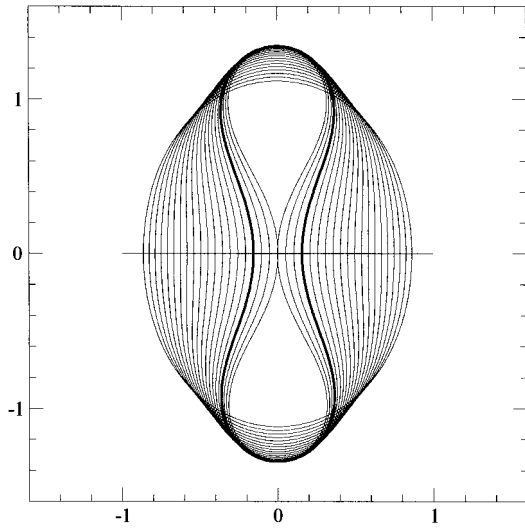


Figure 7. Deformed shapes of a capsule with a biconcave resting shape drawn with the heavy line. The resting shape is described by Equation (2.8) with $\delta = 2$.

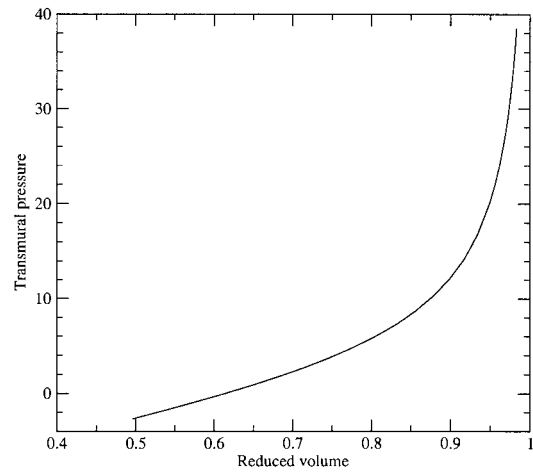


Figure 8. Dimensionless transmural pressure $\Delta \hat{p}_S$ plotted against the reduced capsule volume for the shapes depicted in Figure 7.

Figure 7 shows a family of deformed shapes for a capsule whose resting shape is described by equation (2.8) with $\delta = 2$, for centerline curvature $a_L \kappa_s(0) = -1.3, -1.2, -1.1, -1.0$ (resting shape), $-0.9, \dots, 0.50, 0.60$. The scale has been adjusted so that the shapes displayed have the same surface area. Figure 8 shows the dimensionless transmural pressure $\Delta \hat{p}_S$ plotted against the capsule volume reduced by $4\pi a_S^2$, which is the maximum volume of a spherical capsule with a given surface area. The undeformed shape corresponds to reduced volume of 0.614. In agreement with physical intuition, negative and positive values of the transmural pressure occur, respectively, in the case of deflation or collapse. In particular, as a capsule enclosed by an incompressible membrane is inflated, the internal pressure rapidly escalates toward a large but most certainly finite limit.

4. Discussion

Zarda *et al.* [4] computed the shapes of deflated and inflated capsules with spherical and biconcave resting shapes resembling red blood cells on the basis of the equilibrium equations (2.10)–(2.13) (see also [1]). Their transverse shear tension Q is the negative of the one presently employed, $Q = -q$, and their equilibrium equations are written in terms of the angle θ subtended between the x axis and the normal to the membrane defined such that $d\sigma/ds = \cos \theta$ and $d/ds = \cos \theta(d/d\sigma)$. In their formulation, the principal membrane tensions are given in terms of isotropic and deviatoric components γ and γ' , defined by the equations $\tau_s = \gamma - \gamma'$ and $\tau_\varphi = \gamma + \gamma'$. The isotropic tension is computed to satisfy the inextensibility condition $\lambda_s \lambda_\varphi = 1$, while the deviatoric component derives from a surface strain-energy function W_S as

$$\gamma' \equiv \frac{1}{2}(\tau_s - \tau_\phi) = \frac{1}{2}\left(\frac{1}{\lambda_\phi} \frac{\partial W_S}{\partial \lambda_s} - \frac{1}{\lambda_s} \frac{\partial W_S}{\partial \lambda_\phi}\right). \quad (4.1)$$

Previously, Skalak *et al.* [19] proposed the following strain energy function for the membrane of a red blood cell,

$$W_S = \frac{B}{4}\left(\frac{1}{2}I_1^2 + I_1 - I_2\right) + \frac{C}{8}I_2^2, \quad (4.2)$$

where $I_1 \equiv \lambda_s^2 + \lambda_\phi^2 - 2$ and $I_2 \equiv \lambda_s^2 \lambda_\phi^2 - 1$ are strain invariants, and B and C are physical constants with estimated values on the order of $B \simeq 0.005$ dyn/cm and $C \simeq 100$ dyn/cm. The large magnitude of the constant C compared to that of B ensures that a small deviation of I_2 from unity generates large elastic tensions; consequently, the membrane is nearly incompressible and the tensions are nearly isotropic. To compute equilibrium shapes, Zarda *et al.* [4] traced the membrane contour with marker points and solved the governing equations in an indirect fashion by minimizing a properly constructed energy functional using a finite-element method.

Zarda *et al.* [4] computed shapes of deflated spherical capsules that are qualitative similar with those depicted in our Figure 3(a) (their Figure 8), and presented a graph of the transmural pressure against the capsule volume, as shown in our Figure 6 (their Figure 9). Their results suggest that the transmural pressure diverges to infinity as the reduced volume approaches unity, which means that, if an infinitesimal amount of fluid is withdrawn from the capsule, the internal capsule pressure immediately becomes very large and possibly infinite. This is in contrast with the present results and defies physical intuition.

The results presented in our Figure 7 and 8 are qualitatively similar with those presented in Figures 4 and 5 of Zarda *et al.* [4] for sphered red blood cells. In their Table 1, these authors list the cell volume and transmural pressure for surface area $141.6 \mu\text{m}^2$. The reduced volume of the undeformed shape is 0.58, which is close to the value 0.614 corresponding to the cell depicted in the present Figure 7. Our computations show that, at the reduced volume 0.92, $\Delta \hat{p}_S \simeq 14.5$. Taking as $a_s = 3.36 \mu\text{m}$, corresponding to surface area $141.6 \mu\text{m}^2$, and $E_B = 10^{-12}$ dyn cm, we find the transmural pressure 0.38 dyn cm^2 . Considering the important differences in the constitutive equations for the bending moments and in the assumed resting shapes, this prediction is reasonably close to the value 3.6 dyn/ cm^2 reported by the previous authors [4].

In conclusion, we have formulated a boundary-value problem describing the deformation of axisymmetric capsules enclosed by incompressible membranes developing isotropic tensions due to the deformation from a reference configuration. The constitutive equation for the bending moments was selected so that the principal stretches do not appear in the third-order differential equation for the meridional and azimuthal curvatures in the deformed state. This particular choice, motivated by significant advantages in computational efficiency, is perhaps the most important limitation of the present approach. The development of similar models culminating in computationally amenable elliptic boundary-value problems describing the deformed state of three-dimensional capsules and shells is under current investigation.

References

1. E. A. Evans and R. Skalak, *Mechanics and Thermodynamics of Biomembranes*. Boca Raton, Florida: CRC Press (1980) 254 pp.
2. Y. C. Fung, *Biodynamics: Circulation*. New York: Springer-Verlag (1984) 404 pp.

3. C. Pozrikidis, Effect of bending stiffness on the deformation of liquid capsules in simple shear flow. *J. Fluid Mech.* 440 (2001) 269–291.
4. P. R. Zarda, S. Chien and R. Skalak, Elastic deformations of red blood cells. *J. Biomech.* 10 (1977) 211–221.
5. C. Pozrikidis, *Introduction to Theoretical and Computational Fluid Dynamics*. New York: Oxford University Press (1997) 627 pp.
6. H. Møllmann, *Introduction to the Theory of Thin Shells*. New York: John Wiley & Sons (1981) 181 pp.
7. C. Pozrikidis, *Numerical Computation in Science and Engineering*. New York: Oxford University Press (1998) 675 pp.
8. E. A. Evans and Y. C. Fung, Improved measurements of the erythrocyte geometry. *Microvasc. Res.* 4 (1972) 335–347.
9. E. Reissner, On the theory of thin elastic shells. In: *Contributions to Applied Mechanics*, H. Reissner Anniversary volume. Ann Arbor: J.W. Edwards (1949) 231–247.
10. E. Reissner, On axisymmetrical deformations of thin shells of revolution, proceedings. In: *Third Symposium in Applied Mathematics*. New York: McGraw Hill (1950) 27–52.
11. E. Reissner, On the equations for finite symmetrical deflections of thin shells of revolution. In: *Progress in Applied Mechanics*, Prager Anniversary Volume. New York: McMillan (1963) 171–178.
12. E. Reissner, On finite symmetrical deflections of thin shells of revolution. *J. Appl. Mech.* 36, Trans. ASME 91 Series E (1969) 267–270.
13. D. J. Steigmann, Fluid films with curvature elasticity. *Arch. Rat. Mech.* 150 (1999) 127–152.
14. D. J. Steigmann and R. W. Ogden, Plane deformations of elastic solids with intrinsic boundary elasticity. *Proc. R. Soc. London A* 453 (1997) 853–877.
15. D. J. Steigmann and R. W. Ogden, Elastic surface-substrate interactions. *Proc. R. Soc. London A* 455 (1999) 427–474.
16. J. E. Flaherty, J. B. Keller and S. I. Rubinow, Post-buckling behavior of elastic tubes and rings with opposite sides in contact. *SIAM J. Appl. Math.* 23 (1972) 446–455.
17. C. Pozrikidis, Buckling and collapse of open and closed cylindrical shells. *J. Eng. Math.* 42 (1992) 157–180.
18. N. Yamaki, *Elastic Stability of Circular Cylindrical Shells*. New York: North-Holland (1984) 558 pp.
19. R. Skalak, A. Tözeren, P. R. Zarda and S. Chien, Strain energy function of red blood cell membranes. *Biophys. J.* 13 (1973) 245–264.